Aluminium alloys with transition metals prepared by powder metallurgy

V Kucera[1], F Prusa[1], D Vojtech[1]

[1]Department of Metals and Corrosion Engineering, University of chemistry and technology Prague, Technická 5, 16628 Prague 6, Czech Republic

E-mail: kucerao@vscht.cz

Abstract. Powder metallurgy represented by mechanical alloying and spark plasma sintering was used for preparation of the AlFe16 and the AlSi20Fe16 alloys. Microstructure of the both alloys consisted of very fine intermetallic phases homogenously dispersed in the matrix of α-Al solid solution. Fine nature of microstructure led to promising results of compressive stress-strain tests performed at laboratory and elevated temperature of 400 °C. The compressive strengths of the AlSi20Fe16 and the AlFe16 alloys at laboratory temperature were 780 MPa and 508 MPa, respectively. Elevated temperature resulted in drop of the compressive strengths to 480 MPa and 211 MPa, respectively. However, the results of investigated alloys outperformed the thermally stable AlSi12Cu1Mg1Ni1 (wt. %) used as reference material.

1 Introduction

Aluminium and its alloys belong to the most widespread used metallic materials, especially in automotive or aircraft industry, due to its low density and good strength to weight ratio [1, 2]. The primary production of pure aluminium from ore consumes a huge amount of energy and it is potentially harmful for the environment. Hence, recycling of aluminum alloys becomes more and more important, since it consumes much less energy. The main disadvantage of recycling is the accumulation of the impurities and other alloying elements in the melt [3-5]. It is the iron, which is the common impurity in aluminium alloys and also other transition metals that negatively influences the mechanical properties. In the alloys produced by conventional casting technologies, transition metals form relatively large intermetallic phases due to their low solubility in α-Al solid solution (max. solubility for Fe is 0.052 wt.% at 655 °C) [6]. In the Al-Si-Fe based alloys these intermetallic phases are α-Al_8Fe_2Si with hexagonal structure and monoclinic or orthorhombic β-Al_5FeSi phase, while a monoclinic $Al_{13}Fe_4$, also described in literature as Al_3Fe, is formed in the Al-Fe alloys. The morphology of the phases is needle-like or platelet-like and its dimension depends on the content of the iron as well as on the cooling rate during solidification. The length of β-phase, commonly considered as the most harmful phase in the Al-Si-Fe alloys, increases with iron content. The detrimental effect on mechanical properties, particularly on ductility, is caused by the brittle nature of the phase, which acts as potential site for microcrack propagation and growth resulting in subsequent decohesion failure [6-10]. To prevent the formation of brittle and relatively large intermetallic phases, powder metallurgy is used as an alternative to process aluminium alloys with high content of transition metals [6, 11, 12]. On the other hand, transition metals are characterized with low diffusion coefficients in α-Al solid solution. Therefore, aluminium alloys with high content of these elements are considered as materials for elevated temperatures applications [12, 13]. Thus, the refinement of the potentially harmful phases down to sub-micrometer sizes represents

the way how to utilize such materials, while the mechanical properties can outperform currently used alloys [14].

Mechanical alloying (MA) belongs partially among the severe plastic deformation (SPD) methods. It was originally developed to manufacture oxide-dispersion strengthened (ODS) alloys. However its use is increasing and materials with fully amorphous or nanocrystalline microstructure, disordered solid solutions and supersaturated solid solution are produced by this method. During the MA, particles of the powders are trapped between milling balls and wall of the mill and are repeatedly flattened, cold welded, fractured and re-welded again. Therefore, particles of the powders are heavily deformed, which leads to increase of crystal defects such as vacancies, dislocations, stacking faults and increased number of grain boundaries [15-17]. To preserve fine character of the microstructure obtained by the MA, prepared powders are consolidated via spark plasma sintering (SPS). The SPS is loosely described as control flow of current (up to 20 000 A) throughout a conductive die (mostly fabricated of graphite or WC) filled with powder, which is at the same time compressed by a moving pistons. A high thermal efficiency and heating rate enables consolidation at relatively lower temperatures and reduce the total time of compaction [12, 18].

In this work, two aluminium alloys with high content of iron were prepared by short-term MA and subsequently compacted via SPS. The prepared MA+SPS alloys were investigated to determine the phase composition, microstructure as well as mechanical properties and thermal stability.

2 Materials and methods

The AlFe16 and AlSi20Fe16 (in wt. %) alloys were prepared by short-term MA and compacted via SPS. Pure powders of Al (purity 99.7 %), Fe (purity 99.9 %) and Si (purity 99.9 %) were blended together at the proper ratio and placed into a steel mould together with milling balls both made from AISI 420 stainless steel, sealed and flushed with argon gas to prevent oxidation during alloying. The ball-to-powder mass ratio was 30:1. Mechanical alloying was done by planetary milling device Retsch PM 100 with rotational speed of 400 rpm while the direction of rotation was reversed every 30 min. The total time of MA was 8 hours.

Prepared powder alloys were pre-compacted by the pressure of 360 MPa for 5 minutes at the LabTest 5.250SP1-VM universal testing machine forming semi-compact samples further used for the compaction via SPS. For this purpose, the FCT Systeme HP-D 10 was used. The heating rate was 200 °C·min^{-1} till it reached final 500 °C. After the temperature was reached, the sample was compressed by a pressure of 48 MPa. The total time the sample remained at the 500 °C was 10 minutes followed by a spontaneous cooling.

Simultaneously, both alloys were prepared by common casting metallurgy simulating slow solidification. The AlFe16 alloy was prepared by melting the master alloy AlFe25 (in wt. %) with pure aluminium (purity of 99.62 %) in electric resistance furnace. The melt was casted into a brass mould forming a slowly solidified ingot with 50 mm in diameter and 150 mm in height. The AlSi20Fe16 alloy was prepared by melting pure aluminium and silicon (purity of 99.9%) together with AlFe25 (wt. %) master alloy by induction under a protective argon atmosphere and then poured into a brass mould forming an ingot measuring 20 mm in diameter and 150 mm in height.

Chemical and phase composition was studied by XRF and XRD (ARL 9400 XP and PANalytical X'Pert Pro, Cu Kα1 λ=1.54059·10^{-10} m) analyses.

Compact samples were cut using a cutting machine (Leco Vari/Cut VC-50) equipped with a diamond blade into specimens that were used for further microstructural and mechanical investigations. Samples for microstructure observation were prepared by standard metallography procedure including grinding, polishing and etching the samples in Keller reagent (190 ml distilled water, 5 ml HNO_3, 3 ml HCl, 2 ml HF). Microstructure was observed by optical microscope (Olympus PME-3) and scanning electron microscope (Tescan Vega 3 LMU, 20 kV, SE + BSE detectors) equipped with energy dispersive spectroscopy detector (Oxford Instruments INCA 350, 20 mm^2). The compressive tests were performed by the LabTest universal testing machine (already mentioned) with strain speed

of 1 mm/min at laboratory temperature and at elevated temperature of 400 °C. The height to base ratio of the samples for compressive tests was 1.5:1.

As a reference material, the commercial thermally stable casting AlSi12Cu1Mg1Ni1 (wt. %) alloy, obtained in form of an ingot from our external supplier, was used. The alloy was heat treated by the T6 regime combining solution annealing (510 °C/5 h), water quenching and artificial aging (230 °C/6 h).

3 Results and discussion

3.1 X-ray diffraction analysis of the prepared alloys

The X-ray diffraction patterns of as-mixed powders and both alloys prepared by MA+SPS are shown in **Figure 1**. The phase composition of the AlFe16 as-cast alloy corresponds to the α-Al solid solution and to the most thermally stable intermetallic phase $Al_{13}Fe_4$ (not shown). This concurs with the binary Al-Fe phase diagram, where intermetallic $Al_{13}Fe_4$ phase crystallizes from the melt with 16 wt. % of Fe followed by eutectic reaction L → α-Al + $Al_{13}Fe_4$ at eutectic temperature. [6]. The XRD pattern of as-mixed powders (**Figure 1**a) shows only peaks corresponding to pure Al and Fe. After the MA+SPS of the both materials, slight peak broadening corresponding to grain refinement and to the increase of the internal stresses as well as presence of intermetallic phases is clearly visible. Krasnowski and Kulik [15] observed similar behavior in the MA AlFe20 (at. %) alloy, where supersaturated solid solution α-Al was formed during the first hours of the process. More importantly, the formation of new metastable Al_5Fe_2 phase was observed after 25 hours of MA. In comparison, the alloy containing 15 to 17 at. % Fe developed fully amorphous microstructure after 40 hours of MA.

In case of AlFe16 binary alloy none of new phases were observed after 8 hours of MA. However, after consolidation via SPS intermetallic phase $Al_{13}Fe_4$ was formed and the phase composition of consolidated sample composed of the α-Al solid solution and of intermetallic $Al_{13}Fe_4$ phase. The XRD diffraction pattern of the AlSi20Fe16 alloy is depicted in figure 1b. Phase composition of the as-cast alloys (not shown) consisted of α-Al, Si and intermetallic phases identified as $Al_9Fe_2Si_2$ and Al_3FeSi_2, commonly designated in the Al-Fe-Si ternary phase diagram as τ_6 and τ_4 [19]. As in previous case, XRD diffraction pattern of as-mixed powders contained only peaks of pure Al, Si and Fe which presence partially diminished during the MA+SPS allowing to form the $Al_9Fe_2Si_2$ intermetallic phase.

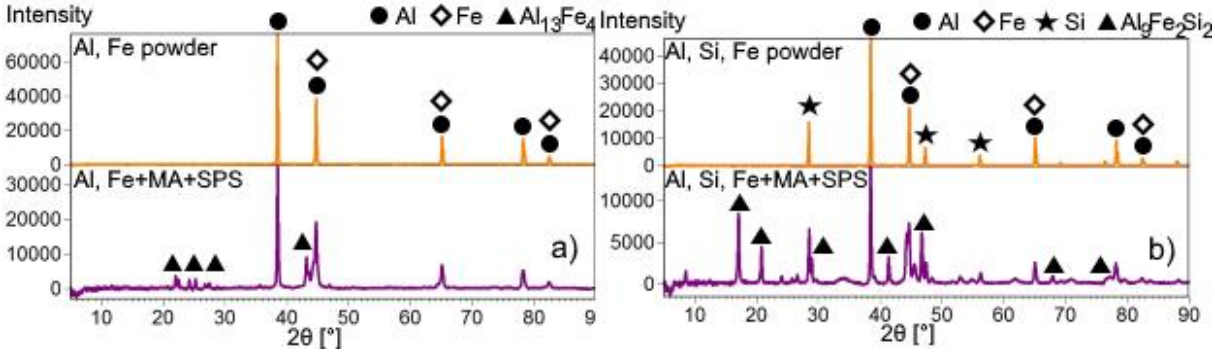

Figure 1. XRD patterns of the as-mixed powders and MA+SPS alloys: a) AlFe16, b) AlSi20Fe16.

3.2 Study of microstructure

The SEM micrographs of the as-cast and MA+SPS alloys are shown in **Figure 2** and **Figure 3**. The microstructure of the both as-cast AlFe16 (**Figure 2**a) and AlSi20Fe16 (**Figure 3**a) alloys was characterized by presence of relatively large intermetallic phases with the longitudinal size reaching several hundreds of micrometres identified as $Al_{13}Fe_4$ (Figure 2a) and $Al_9Fe_2Si_2$, Al_3FeSi_2 (Figure 3a), respectively. Further, the microstructures of both the AlFe16 and AlSi20Fe16 alloys contained eutectic

mixture of α-Al + $Al_{13}Fe_4$ and α-Al + Si, respectively. Furthermore particles of primary silicon are seen in the microstructure of AlSi20Fe16, which is predictable due to the high content of Si. Microstructure of both the MA+SPS alloys consists of very fine intermetallic $Al_{13}Fe_4$ (**Figure 2**b) and $Al_9Fe_2Si_2$ (**Figure 3**b) phases and of very fine particles of Si, which were homogenously dispersed in the α-Al solid solution.

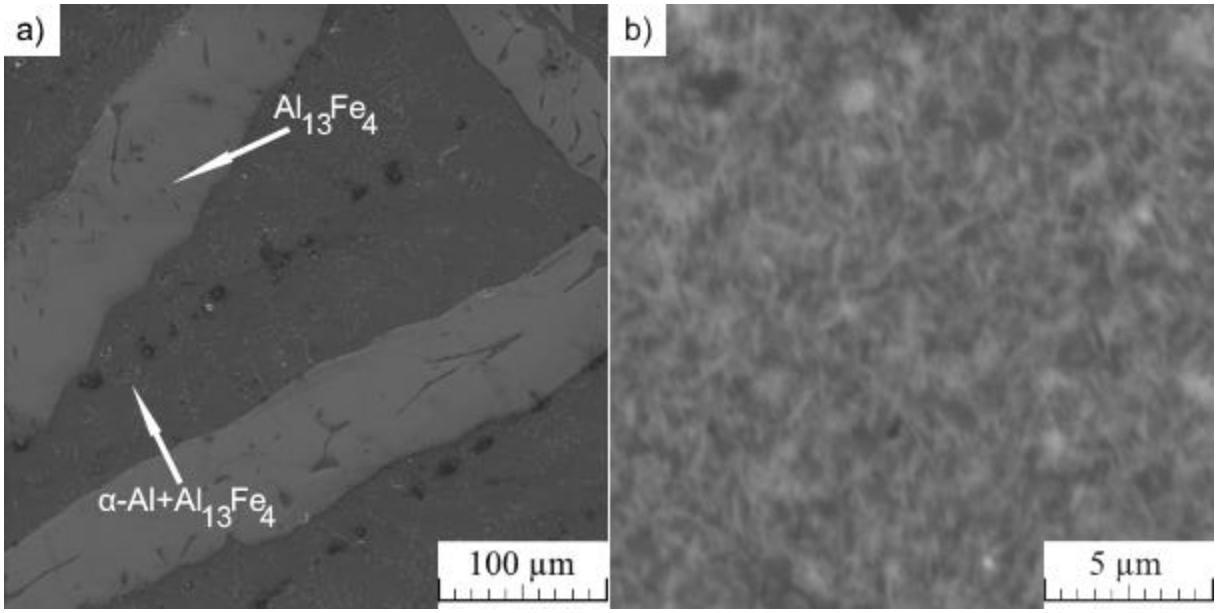

Figure 2. SEM micrographs of AlFe16 alloy: a) as-cast, b) MA+SPS.

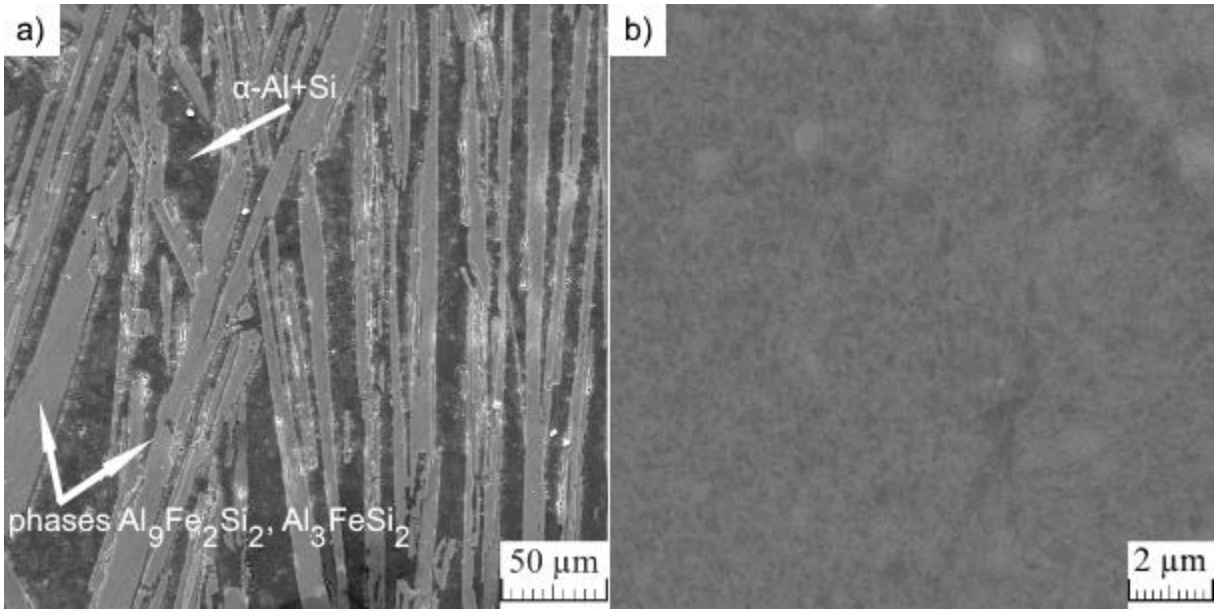

Figure 3. SEM micrographs of AlSi20Fe16 alloy: a) as-cast, b) MA+SPS.

3.3 Compressive stress-strain tests

The compressive stress-strain tests of the MA+SPS alloys were measured at laboratory and elevated temperature of 400 °C and compared to the commercial thermally stable casting AlSi12Cu1Mg1Ni1 alloy. The results are shown in **Figure 4** and in **Table 1**, respectively. The highest compressive strength

(CS) measured at laboratory temperature Figure 4a) was observed by the AlSi20Fe16 alloy reaching 758 MPa. The CS of the MA+SPS AlFe16 alloy was similar to the reference AlSi12Cu1Mg1Ni1 alloy. However, both alloys prepared by MA+SPS exhibited lower plasticity compared to the reference alloy, which can be explained by large internal stresses and strains of the crystallographic lattice induced during the MA and also by a relatively high volume fraction of intermetallic phases as well as by very fine character of present α-Al grains. Figure 4b depicts compressive stress-strain curves at 400 °C. The values of CS could not be determined due to the continuous character of the deformation with absence of fracture. Both the MA+SPS alloys indicated that high value of iron plays important role in thermal stability due to its low diffusion coefficient in α-Al. Compressive yield strength (CYS) of the MA+SPS AlFe16 and AlSi20Fe16 alloys were 211 MPa and 480 MPa, respectively. Such a high value of CYS in the later mentioned alloy was caused by high content of Si particles as well as by high volume fraction of intermetallic phases containing Fe and Si. Thus, both MA+SPS prepared alloys evinced better thermal stability compared to reference AlSi12Cu1Mg1Ni1 alloy that reached CYS of only 100 MPa. Another fact that should be mentioned is the enormous increase in plastic deformation reaching several tens of percent.

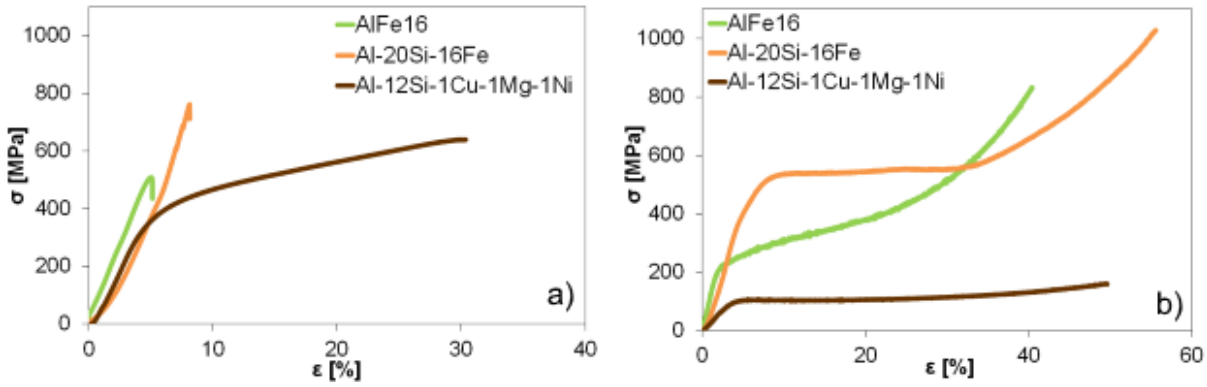

Figure 4. The compression stress-strain curves of tested alloys at laboratory temperature a) and elevated temperature of 400 °C b).

Table 1. Results from compression tests measured at laboratory and elevated temperature of 400 °C (CYS-compressive yield strength; CS-compressive strength).

Sample	Lab. temperature		400 °C	
	CYS [MPa]	CS[MPa]	CYS [MPa]	CS [MPa]
AlFe16	-	508	211	-
AlSi20Fe16	-	758	480	-
AlSi12Cu1Mg1Ni1	430	680	100	-

4 Conclusion

Two aluminium alloys AlFe16 and AlSi20Fe16 were prepared by MA followed by consolidation via SPS. Microstructure of both the MA+SPS alloys consisted of very fine intermetallic phases identified as $Al_{13}Fe_4$ and $Al_9Fe_2Si_2$, respectively, homogenously dispersed in α-Al solid solution. The fine character of the microstructure led to very promising mechanical properties. The highest value of CS (758 MPa) at laboratory temperature was achieved by the Al20Si16Fe alloy, however it showed absence of plastic deformation. Both alloys showed improved thermal stability compared to the reference casting AlSi12Cu1Mg1Ni1 alloy. In fact, the CYS of the MA+SPS AlFe16 alloy was almost two times higher compared to the reference alloy while the AlSi20Fe16 alloy showed almost five times higher CYS.

Acknowledgment
The authors wish to thank the Czech Science Foundation (project no. P108/12/G043) for its financial support of this research.

References

[1] Park W-W, B-S You and N J Kim 1996 *Materials & Design* **17**(5): p. 255-259.
[2] Choi Y S, et al. 1999 *Journal of Materials Science* **34**(9): p. 2163-2168.
[3] Schmitz C, J Domagala and P Haag, *Handbook of Aluminium Recycling*, ed. C. Schmitz. 2007: Vulkan-Verlag GmbH.
[4] Osawa Y, et al. 2007 *MATERIALS TRANSACTIONS* **48**(9): p. 2467-2475.
[5] Malakhov D V, D Panahi and M Gallerneault 2010 *Calphad* **34**(2): p. 159-166.
[6] Belov N A, A A Aksenov and D G Eskin, *Advances in Metallic Alloys*. Iron in Aluminium Alloys: Impurity and Alloying Element, ed. J.N. Fridlyander and D.G. Eskin. Vol. 2. 2002: Taylor & Francis. 360.
[7] Fang X, et al. 2007 *Materials Science and Engineering: A* **445–446**: p. 65-72.
[8] Eidhed W 2008 *Journal of Materials Science & Technology* **24**(1): p. 45 - 47.
[9] Taylor J A 2012 *Procedia Materials Science* **1**: p. 19-33.
[10] Khalifa W, et al. 2005 *Metallurgical and Materials Transactions A* **36**(4): p. 1017-1032.
[11] Dobromyslov A V, et al. 2015 *The Physics of Metals and Metallography* **116**(9): p. 942-950.
[12] Sasaki T T, T Ohkubo and K Hono 2009 *Acta Materialia* **57**(12): p. 3529-3538.
[13] Průša F and D Vojtěch 2013 *Materials Science and Engineering: A* **565**: p. 13-20.
[14] Průša F, et al. 2014 *Materials Science and Engineering: A* **603**: p. 141-149.
[15] Krasnowski M and T Kulik 2009 *Materials Chemistry and Physics* **116**(2–3): p. 631-637.
[16] Minamino Y, et al. 2004 *Science and Technology of Advanced Materials* **5**(1–2): p. 133-143.
[17] Suryanarayana C 2001 *Progress in Materials Science* **46**(1–2): p. 1-184.
[18] Suárez M, et al., *Challenges and Opportunities for Spark Plasma Sintering: A Key Technology for a New Generation of Materials*, in *Sintering Applications*, B. Ertuğ, Editor. 2013, InTech.
[19] Marker M C J, et al. 2011 *Intermetallics* **19**(12): p. 1919-1929.